18. J. O. Calvo and L. Salgado, *Gaia* **11**, 13 (1995).
19. R. Lavocat, *C. R. 19th Int. Geol. Congr.* **3**, 65 (1954).
20. L. L. Jacobs, D. A. Winkler, W. R. Downs, E. M. Gomani, *Palaeontology* **36**, 523 (1993).
21. E. Stromer, *Abh. Bayer. Akad. Wiss. Math. Naturwiss. Abt.* **22**, 1 (1934).
22. Age rank was established with the midpoint of the first stage (or longer temporal unit) in which the taxon has been recorded. Midpoint values were calculated from a recent time scale (*33*). Age rank was scaled from 0 to 1.
23. Clade rank (*26*) was established with recent phylogenetic analyses for Dinosauria (*4*, *9*) with a few terminal taxa collapsed or omitted to achieve single most parsimonious, fully asymmetric cladograms. Clade rank was scaled from 0 to 1.
24. Only unambiguous character-state changes are plotted. If there was no missing ancestral lineage between two or more nodes on the tree (that is, 0 duration), synapomorphies were added to those associated with the next positive duration [method 2 of (*28*)].
25. The minimum duration for missing ancestral lineages ["ghost taxa"; M. A. Norell, *Am. J. Sci.* **293A**, 407 (1993)] was calculated by subtracting the midpoints of the first occurrence dates at successive nodes.
26. J. A. Gauthier, A. J. Kluge, T. Rowe, *Cladistics* **4**, 105 (1988); M. A. Norell and M. J. Novacek, *Cladistics* **8**, 319 (1992).
27. A. B. Smith, B. Lafay, R. Christen, *Philos. Trans. R. Soc. London Ser. B Biol. Sci.* **338**, 365 (1992).
28. C. A. Sidor and J. A. Hopson, *Paleobiology* **24**, 254 (1998); P. J. Wagner and C. A. Sidor, *Syst. Biol.*, in press.
29. The greatest missing lineages in higher level sauropod phylogeny occur at the base of sauropod phylogeny, but most of the terminal taxa (except *Shunosaurus*) still appear successively in time. Spearman rank correlation (corrected for ties) is positive ($S = 0.603$) and significant ($P = 0.0035$).
30. D. L. Fox, D. C. Fisher, L. R. Leighton, *Science* **284**, 1816 (1999).
31. In higher level sauropod phylogeny, missing temporal lineages are shortest or nonexistent at the base of the neosauropod radiation, where a greater amount of skeletal change is known to have occurred. Within Sauropoda, skeletal change is not positively correlated with the duration of missing lineages or significant [Spearman rank correlation (corrected for ties) is negative ($S = -1.00$, $P = 0.1573$)].
32. An alternative data matrix for tetanuran theropods [T. R. Holtz Jr., *J. Paleontol.* **68**, 1100 (1994)] was sampled with some terminal taxa collapsed or omitted to achieve a single most parsimonious cladogram. No iteration could produce a positive or significant correlation between the number of unambiguous synapomorphies and estimated elapsed time.
33. F. M. Gradstein *et al.*, *Soc. Econ. Paleontol. Mineral. Spec. Publ.* **54**, 95 (1995).
34. A. G. Smith, D. G. Smith, B. M. Funnell, *Atlas of Mesozoic and Cenozoic Coastlines* (Cambridge Univ. Press, Cambridge, 1994).
35. Y. Zhang, *The Middle Jurassic Dinosaur Fauna from Dashanpu, Zigong, Sichuan* (Sichuan Publishing House of Science Technology, Chengdu, China, 1988).
36. J. S. McIntosh, C. A. Miles, K. C. Cloward, J. R. Parker, *Bull. Gunma Mus. Nat. Hist.* **1**, 1 (1996).
37. C. W. Gilmore, *Mem. Carnegie Mus.* **10**, 347 (1925).
38. Supported by the David and Lucile Packard Foundation, the National Geographic Society, the Pritzker Foundation, and the Women's Board of the University of Chicago. We thank C. Abraczinskas for drawing original specimens and executing the final drafts of all other figures; Q. Cao, D. Blackburn, J. Conrad, E. Dong, J. Komar, E. Love, C. Noto, and volunteer staff for fossil preparation and casting; and J. Conrad, J. Hopson, and F. Lando for reviewing an earlier draft of this report. We acknowledge the assistance of I. Kouada and B. Gado of the Ministère de L'Enseignement Supérieur de la Recherche et de la Technologie and Institut de Recherches en Sciences Humaine, respectively (Niger). For permission to conduct field work, we are indebted to the Republique du Niger.

8 September 1999; accepted 19 October 1999

Prolonged Activation of Mitochondrial Conductances During Synaptic Transmission

Elizabeth A. Jonas,[1] JoAnn Buchanan,[2] Leonard K. Kaczmarek[1]*

Although ion channels have been detected in mitochondria, scientists have not been able to record ion transport in mitochondria of intact cells. A variation of the patch clamp technique was used to record ion channel activity from intracellular organelles in the presynaptic terminal of the squid. Electron microscopy indicated that mitochondria are numerous in this terminal and are the only organelles compatible with the tips of the pipettes. Before synaptic stimulation, channel activity was infrequent and its conductance was small, although large conductances (~0.5 to 2.5 nanosiemens) could be detected occasionally. During a train of action potentials, the conductance of the mitochondrial membrane increased up to 60-fold. The conductance increased after a delay of several hundred milliseconds and continued to increase after stimulation had stopped. Recovery occurred over tens of seconds.

Intracellular calcium stores are important in the function of excitable cells (*1*, *2*). For example, mitochondrial calcium uptake followed by rapid re-release from the mitochondrial matrix shapes the time course of calcium transients during synaptic activity and prolongs the elevated levels of intracellular calcium (also called "residual calcium") that underlie post-tetanic potentiation (PTP) (*3*).

Mitochondria take up calcium in response to localized elevations in calcium (*4*). Extrusion of protons from the inner mitochondrial matrix produces a large (−160 to −200 mV) voltage gradient across the inner mitochondrial membrane (*5*). Calcium can therefore flow readily along its electrochemical gradient into the mitochondrial matrix (*6*). At rest, the level of free calcium in the matrix is similar to the cytosolic level, but total mitochondrial calcium can increase markedly during depolarization (*2*, *7*). High levels of intramitochondrial calcium interact with matrix enzymes and then exit rapidly, which allows the mitochondria to regain their pre-stimulation levels within 5 min of a cytosolic load (*2*, *8*).

Studies on isolated mitochondria or artificial lipid bilayer preparations have revealed several types of ion channels on both inner and outer mitochondrial membranes (*9*–*13*). However, no technique was available to record ion channel activity from intracellular membranes in intact cells. We have recently described the use of such a technique (*14*), and we have applied it here to the giant presynaptic terminal of the squid.

With electron microscopy, we determined that the dominant structures in the central region of the presynaptic terminal are mitochondria and neurofilaments (Fig. 1) (*15*). Clusters of synaptic vesicles occur at active zones and, occasionally, in more central regions. Vesicle size (50 nm) is too small, however, to allow seal formation across the tips of the pipettes. Thin strips of membranes, possibly from endoplasmic reticula, could also be detected sometimes but accounted for less than ~2% of the internal membranes. Thus the mitochondria (Fig. 1), whose cross-sectional diameters range from ~300 to 1200 nm [mean = 575 ± 181 (SD) nm, $n = 15$] are the only internal organelles that are compatible with seal formation by the patch pipettes, which have tip diameters of ~180 to 200 nm (*16*).

Seals (0.5 to 6.0 gigohm) were obtained in 94 experiments using the technique in (*17*); 71 of the 94 seals were greater than 1.5 gigohm. The successful recordings represented approximately 40% of attempts. When a fluorescent lipophilic dye was included in the patch pipette, a fluorescent signal could be detected only after a high-resistance seal was obtained ($n = 7$). The fluorescent signals in all the dye experiments were located within the large terminal finger of the presynaptic terminal (*18*).

After formation of a gigohm seal, the potential of the patch was set between −100 and +100 mV to record the spontaneous and voltage-dependent activity in the membranes. We observed spontaneous channel activity in 50% of the seals ($n = 47$ out of 94) and the amplitude of such activity was usually low. In many

[1]Department of Pharmacology, Yale University School of Medicine, New Haven, CT 06520, USA. [2]Department of Molecular and Cellular Physiology, Stanford University Medical Center, Stanford, CA 94305, USA.

*To whom correspondence should be addressed. E-mail: leonard.kaczmarek@yale.edu

cases, unitary openings of 2 to 4 pA at +100 mV were detected. These openings occurred infrequently and were difficult to detect at multiple potentials. In 11 experiments, however, more frequent openings were detected at all potentials (Fig. 2). The current-voltage plot in Fig. 2B summarizes data from these 11 channels. A large voltage-dependent conductance was also observed (n = 5) (Fig. 2C). A striking characteristic of this type of channel is that it opened only after repeated depolarizations of the patch, usually to pipette potentials >+40 mV (Fig. 2D). The conductances of these channels ranged from 0.5 to 2.5 nS with multiple subconductance states and could be observed in the same patches that also contained the smaller conductance activity.

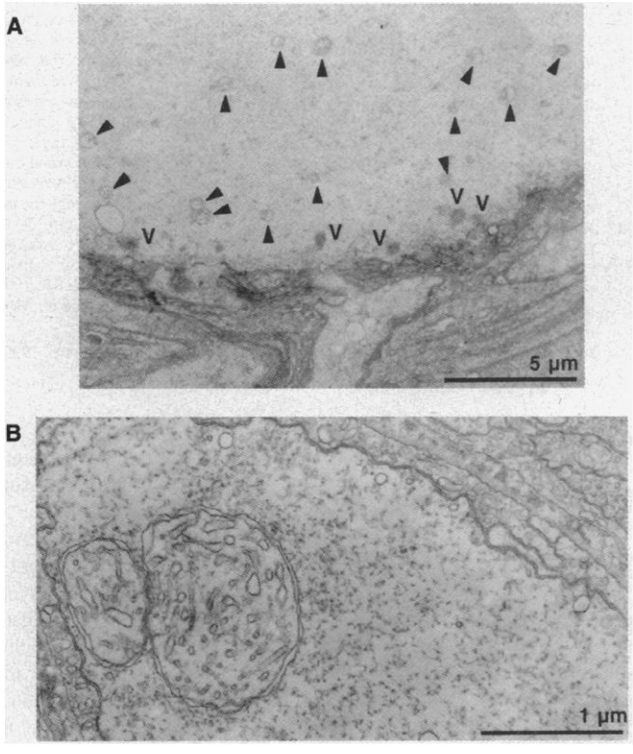

Fig. 1. Mitochondria in the squid presynaptic terminal. (**A**) Electron micrograph of a section of a squid presynaptic terminal. Mitochondria in the central region of the terminal are indicated by arrows. Clusters of synaptic vesicles (V) are adjacent to the presynaptic plasma membrane where it contacts the postsynaptic axon. Internal membranes are denser in the postsynaptic axon, which is seen at the bottom of the micrograph. (**B**) View of mitochondria and neurofilaments in the presynaptic terminal at higher power.

Next we stimulated the presynaptic terminal while recording from an intracellular patch. Trains of action potentials were elicited at 20 Hz for several seconds, and parallel experiments showed that synaptic transmission was maintained throughout these trains (*19*). Figure 3A shows the change in conductance of an intracellular membrane seal during synaptic transmission. Before stimulation, infrequent small-conductance channels were observed. Activity increased markedly in 17 of 26 stimulated termini during the stimulus train. After stimulation of the presynaptic nerve ceased, the enhanced activity continued and, in many cases, increased in amplitude for several seconds (Fig. 4). Activity gradually decreased in frequency and in amplitude over the following 5 to 30 s (Figs. 3B and 4). After the first presynaptic stimulus, the time to onset of increased activity was 0.726 ± 0.183 s (n = 7).

The increased channel activity on the intracellular membrane did not occur simultaneously with the opening of the plasma membrane channels. It did outlast action potential firing, which suggests that the activity might depend on an intracellular second messenger. During synaptic stimulation, there is a buildup of calcium in the presynaptic terminal (*3*). We eliminated calcium from the external medium and recorded channel activity from intracellular membranes as before. There was no response to stimulation of the presynaptic terminal in a calcium-deficient bathing medium (Fig. 3C)

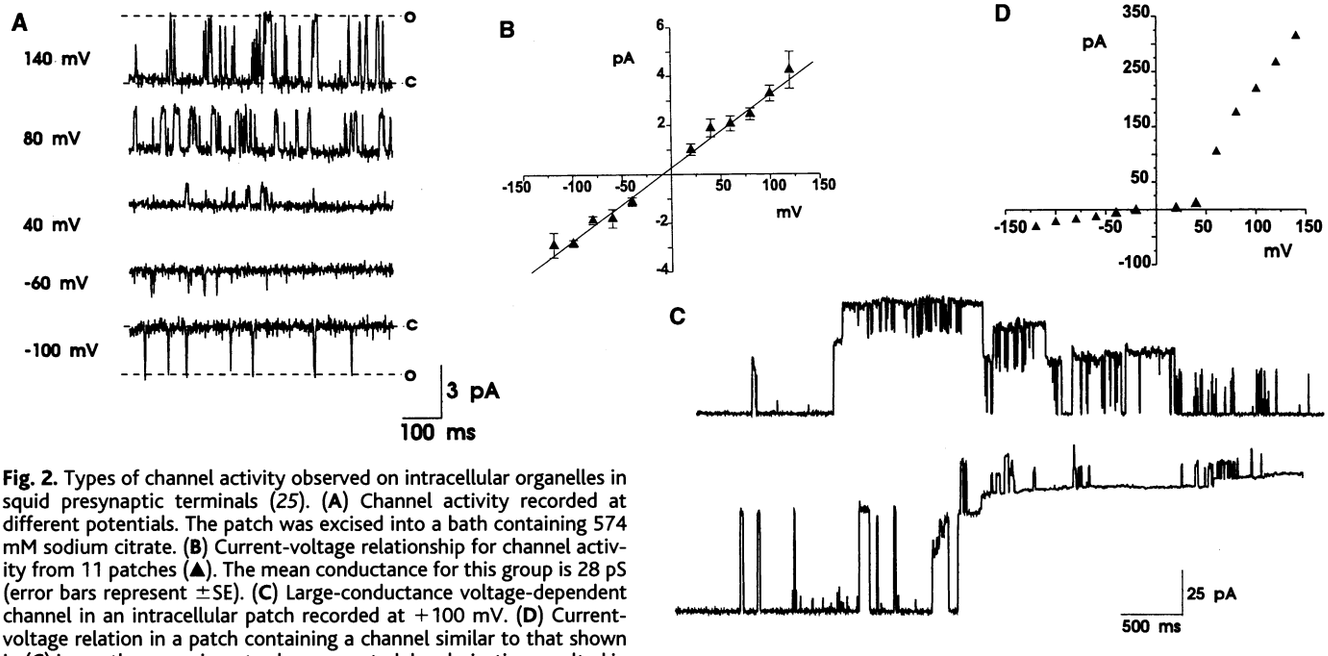

Fig. 2. Types of channel activity observed on intracellular organelles in squid presynaptic terminals (*25*). (**A**) Channel activity recorded at different potentials. The patch was excised into a bath containing 574 mM sodium citrate. (**B**) Current-voltage relationship for channel activity from 11 patches (▲). The mean conductance for this group is 28 pS (error bars represent ±SE). (**C**) Large-conductance voltage-dependent channel in an intracellular patch recorded at +100 mV. (**D**) Current-voltage relation in a patch containing a channel similar to that shown in (C) in another experiment, where repeated depolarization resulted in activation of a large (2.5 nS) conductance channel at depolarized potentials. Currents plotted (▲) represent total patch current. Discernible openings of the large conductance channel were detected only at potentials >+40 mV.

(n = 5). In addition, experiments were carried out after treatment of the ganglia with the mitochondrial uncoupling agent FCCP (carbonyl cyanide p-trifluoromethoxyphenylhydrazone; 10 μM solution for 20 min), which also eliminated the increase in conductance upon stimulation (n = 6). FCCP also eliminated potentiation of synaptic responses after stimulation in a 1.75 mM external Ca^{2+} bathing medium (n = 4) (*20*).

To determine whether the increased activity was restricted to the presynaptic terminal, we compared these results to those obtained from recordings within the postsynaptic cell. Seals within the postsynaptic axon did not respond to stimulation (n = 5), which suggests that this enhanced activity mostly occurs at the presynaptic site (Fig. 3D).

Several discrete levels of conductance were detected. Further analysis of the timing of the onset of the increased conductances for one presynaptic patch is shown in Fig. 4, A and B. Small-conductance activity (~28 pS) was present before stimulation (Fig. 4A, top). The conductance increased during stimulation and increased even more after stimulation ceased, as larger conductance levels were recruited into the patch. The total conductance gradually decreased, eventually leaving the patch quiescent about 15 to 30 s after stimulation. The corresponding amplitude histograms are shown in Fig. 4B. In some experiments, the progressive increase in conductance occurred in several discrete bursts, after which the membrane returned to its quiescent state (*18*). The appearance of larger conductances or bursts or both may reflect the recruitment of additional channels or changes in the gating behavior of channels already active in the patch.

The current-voltage plot for a patch before and after a train of action potentials is shown in Fig. 4C. Before stimulation, a conductance of

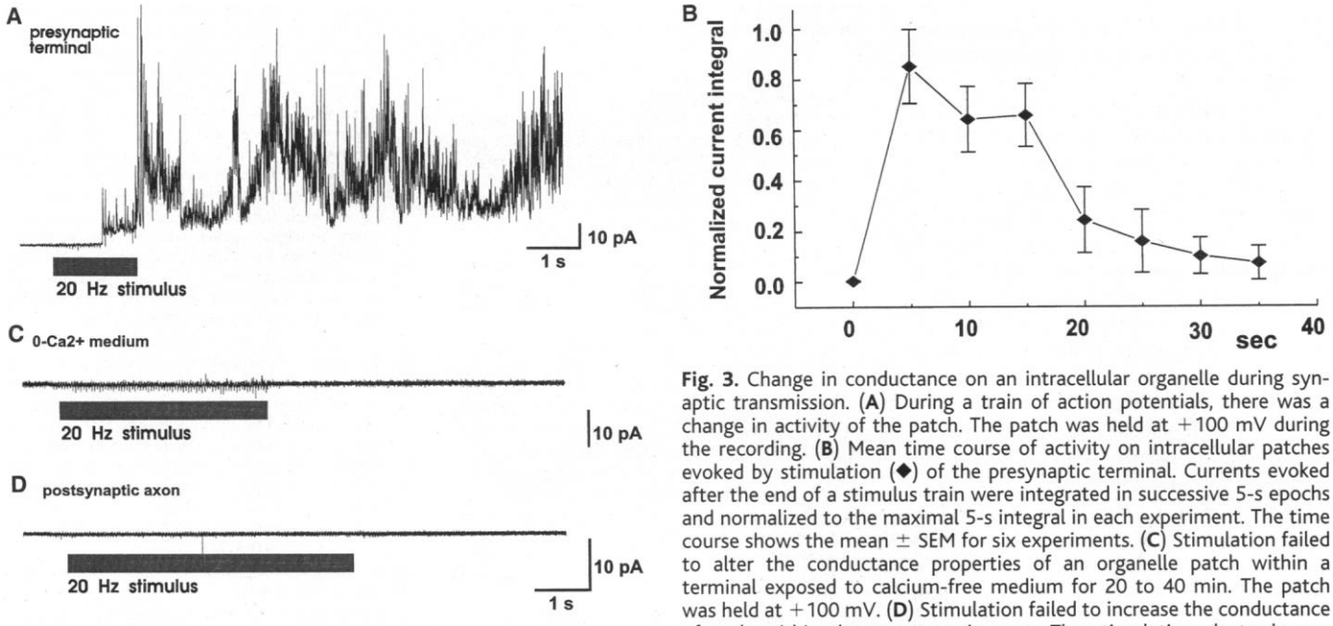

Fig. 3. Change in conductance on an intracellular organelle during synaptic transmission. (**A**) During a train of action potentials, there was a change in activity of the patch. The patch was held at +100 mV during the recording. (**B**) Mean time course of activity on intracellular patches evoked by stimulation (◆) of the presynaptic terminal. Currents evoked after the end of a stimulus train were integrated in successive 5-s epochs and normalized to the maximal 5-s integral in each experiment. The time course shows the mean ± SEM for six experiments. (**C**) Stimulation failed to alter the conductance properties of an organelle patch within a terminal exposed to calcium-free medium for 20 to 40 min. The patch was held at +100 mV. (**D**) Stimulation failed to increase the conductance of seals within the postsynaptic axon. The stimulating electrode was placed on the presynaptic nerve (n = 4), or the postsynaptic axon (n = 1). The patch was held at +100 mV.

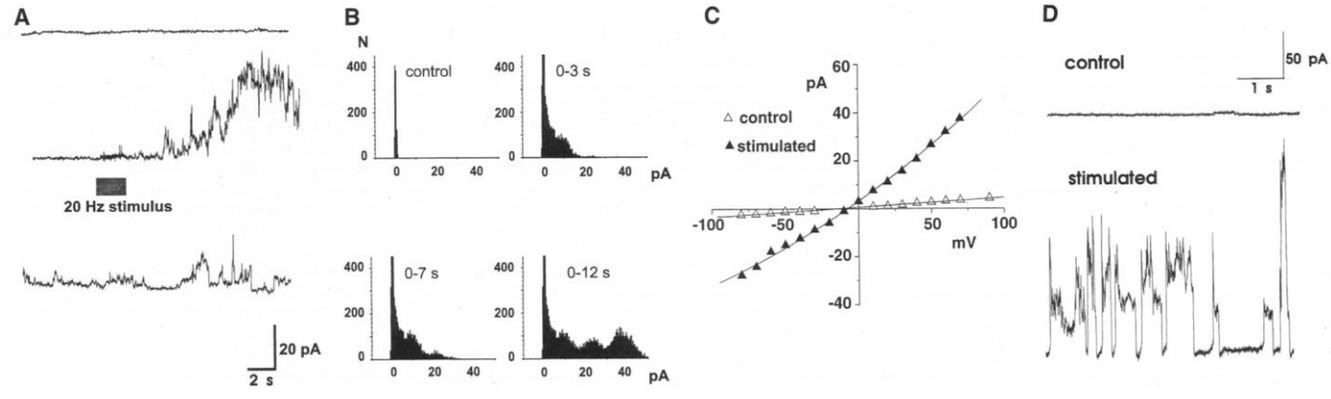

Fig. 4. Increasing amplitude conductances recruited after stimulation. (**A**) Conductance changes in a patch during and after stimulation of the presynaptic nerve. Before stimulation, there is no large-conductance activity (upper trace), but recruitment of larger conductances occurs over the first 15 s after stimulation (middle trace), immediately followed by a decrease in activity (bottom trace). The patch was held at +100 mV. (**B**) Successive amplitude histograms of data shown in (A). Progressive recruitment of discrete peaks of larger conductances is evident. (**C**) Typical current-voltage relation for an evoked response obtained from an on-organelle patch. Control currents represent the measurements of the openings of the small-conductance channel in the patch. Currents evoked after repeated stimulation of the presynaptic nerve represent total patch current, after subtraction of leak current that was measured before stimulation. (**D**) Depolarization-sensitive channel openings in a stimulated patch. Recordings are at +100 mV in the control (before stimulation, upper panel) and after stimulation (lower panel). Activity after stimulation was evident only at depolarized potentials, similar to the channel activity shown in Fig. 2, C and D. A small-conductance opening can be seen in the prestimulation recording.

~28 pS was observed. After stimulation, the peak conductance was 420 pS, and the current-voltage relationship remained linear. Ion substitution experiments on such patches that had been excised after stimulation indicated that the peak conductance was largely carried by cations, and that potassium was slightly more permeant than sodium (*18*). In other experiments ($n = 4$), stimulation triggered the activation of a voltage-sensitive channel (Fig. 4D). Before stimulation, only small-conductance infrequent openings were observed. After stimulation, large multiple-conductance activity of up to 2.5 nS was observed upon depolarization of the patch. The voltage dependence of these channels appeared to be identical to the channels presented in Fig. 2D; that is, the channel openings were detected only at potentials positive to +40 mV.

There is a large increase in conductance on intracellular membranes in response to synaptic activity, and this change depends on the presence of extracellular calcium. The conductance change may result from the combined activity of several ion channel types. Because the voltage-dependent anion channel (VDAC) is the predominant protein in the outer mitochondrial membrane, it is possible that this protein contributes to the activation of the conductance we observed during synaptic transmission. In reconstitution experiments, VDAC has wide ion selectivity with multiple conductances of up to 4 nS (*10*). A channel with a strong voltage dependence similar to that shown in Fig. 2D has been detected in recordings of inner mitochondrial membranes (*11*). Openings of this channel, however, occurred upon depolarization of the mitochondrial membrane, whereas a positive patch potential in our experiments would be expected to hyperpolarize intact mitochondria. Thus, it is possible that in experiments in which the large-conductance voltage-dependent channel was detected, recordings were made in the "whole-organelle" configuration. Rigorous comparisons are, however, difficult because the properties of an ion channel recorded on the membrane of an organelle in situ may differ from that of the same channel expressed in bilayers or on an isolated organelle. For example, the conductance of VDAC has been shown to be affected by enzymes present in the intermembrane space (*21*). Moreover, the membrane potential across the patches in our experiments is not known, and apparent conductance may also be altered by the capacitance and resistance of the organelle itself and by local ion concentrations.

The conductance change during synaptic stimulation depends on calcium entry into the terminal. It is possible that this change reflects calcium entry into the inner matrix of the mitochondria. Under some experimental conditions, calcium permeability of the inner mitochondrial membrane is sensitive to elevated levels of matrix calcium (*12*). Permeability may also be increased by mitochondrial membrane depolarization (*22*) and by matrix alkalinization (*23*), both of which occur when calcium enters the mitochondria. The inner and outer membranes form linkages at contact sites, which may couple the activity of channels in the two membranes (*24*). Thus it is possible that inner membrane activity could be recorded with the patch pipette on the outer membrane.

The facts that the calcium-dependent change in mitochondrial conductance we have described outlasts the period of stimulation and that its time course closely matches that of post-tetanic potentiation, a phenomenon that requires mitochondrial integrity (*3*), suggest that the activation of mitochondrial conductances contributes to synaptic plasticity.

References and Notes

1. S. L. Budd and D. G. Nicholls, *J. Neurochem.* **66**, 403 (1996); J. Herrington, Y. B. Park, D. F. Babcock, B. Hille, *Neuron* **16**, 219 (1996); D. F. Babcock, J. Herrington, P. C. Goodwin, Y. B. Park, B. Hille, *J. Cell Biol.* **136**, 833 (1997); Y.-Y. Peng, *J. Neurophysiol.* **80**, 186 (1998).
2. N. B. Pivovarova, J. Hongpaisan, S. B. Andrews, D. D. Friel, *J. Gen. Physiol.* **111**, 39a (1998).
3. D. D. Friel and R. W. Tsien, *J. Neurosci.* **14**, 4007 (1994); Y.-g. Tang and R. S. Zucker, *Neuron* **18**, 483 (1997); D. F. Babcock and B. Hille, *Curr. Opin. Neurobiol.* **8**, 398 (1998).
4. A. L. Lehninger, *Biochem. J.* **119**, 129 (1970); R. Rizzuto, M. Brini, M. Murgia, T. Pozzan, *Science* **262**, 744 (1993); L. S. Jouaville, F. Ichas, E. L. Holmuhamedov, P. Camacho, J. D. Lechleiter, *Nature* **377**, 438 (1995); R. Rizzuto *et al.*, *Science* **280**, 1763 (1998); F. Ichas, L. S. Jouaville, J.-P. Mazat, *Cell* **89**, 1145 (1997).
5. P. Mitchell, *Nature* **191**, 144 (1961); T. E. Gunter and D. R. Pfeiffer, *Am. J. Physiol.* **258**, C755 (1990).
6. G. C. Sparagna, K. K. Gunter, S.-S. Sheu, T. E. Gunter, *J. Biol. Chem.* **270**, 27510 (1995).
7. H. Miyata *et al.*, *Am. J. Physiol.* **261**, H1123 (1991); R. Rizzuto, A. W. M. Simpson, M. Brini, T. Pozzan, *Nature* **358**, 325 (1992).
8. R. M. Denton and J. G. McCormack, *Annu. Rev. Physiol.* **52**, 451 (1990); W.-F. Pralong, A. Spat, C. B. Wollheim, *J. Biol. Chem.* **269**, 27310 (1994).
9. K. W. Kinnally and H. Tedeschi, in *Molecular Biology of Mitochondrial Transport Systems*, M. Forte and M. Colombini, Eds. (Springer-Verlag, Berlin, 1994), pp. 169–198; M. C. Sorgato and O. Moran, *Crit. Rev. Biochem. Mol. Biol.* **28**, 127 (1993).
10. M. Colombini, E. Blachly-Dyson, M. Forte, in *Ion Channels*, T. Narahashi, Ed. (Plenum, New York, 1996), vol. 4, pp. 169–202; T. Rostovtseva and M. Colombini, *J. Biol. Chem.* **271**, 28006 (1996); I. Hodge and M. Colombini, *J. Membr. Biol.* **157**, 271 (1997).
11. M. C. Sorgato, B. U. Keller, W. Stuhmer, *Nature* **330**, 498 (1987).
12. V. Petronilli, I. Szabo, M. Zoratti, *FEBS Lett.* **259**, 137 (1989); K. W. Kinnally, D. B. Zorov, Y. N. Antonenko, S. Perini, *Biochem. Biophys. Res. Comm.* **176**, 1183 (1991); I. Szabo, P. Bernardi, M. Zoratti, *J. Biol. Chem.* **267**, 2940 (1992).
13. P. Juin, M. Thieffry, J.-P. Henry, F. M. Vallette, *J. Biol. Chem.* **272**, 6044 (1997); G. Schatz, *Nature* **395**, 439 (1998); K. Hill *et al.*, *Nature* **395**, 516 (1998); K.-P. Kunkele *et al.*, *Cell* **93**, 1009 (1998).
14. E. A. Jonas, R. J. Knox, L. K. Kaczmarek, *Neuron* **19**, 7 (1997).
15. Stellate ganglia were fixed in glutaraldehyde (2%) and 2.5% paraformaldehyde in 0.1 M cacodylate buffer, pH 7.4, that contained 0.8 M sucrose. They were then post-fixed for 30 min in 2% osmium tetroxide in 0.1 M cacodylate buffer with 0.8 M sucrose, during which time they were microwaved for short bursts. They were dehydrated and infiltrated in the microwave, then flat embedded in Embed 812 (Electron Microscopy Sciences, Fort Washington, PA). Sections 2 μm thick were cut until the synapse was located, after which 50-nm thin sections were cut. The sections were contrasted with uranyl acetate and lead nitrate and were examined with a Phillips CM12 electron microscope at 60 kV.
16. The size of pipette tips was determined by scanning electron microscopy (SEM) (*18*).
17. Intracellular membrane recordings were performed according to the method of Jonas *et al.* (*14*). The intracellular membrane pipette (20 to 80 megohms) was pulled on a Sutter Instruments P87 puller (Novato, CA), then fire-polished. Pipettes were filled with molluscan intracellular solution (pH 7.2), which contained the following: 480 mM KCl, 11 mM $MgCl_2$, 10 mM Hepes, 70 mM EGTA, 43 mM $CaCl_2$, and 2 mM ATP, or a similar solution where K aspartate was substituted for KCl. The inner electrode was mounted in a standard electrode holder with a side port attached to manual suction. The outer electrode was made of softer, larger-bore glass, not polished, and only the tip was filled with intracellular solution. The inner electrode was manually inserted into the outer electrode, and microscope oil was placed between the two electrodes. The inner and outer electrodes were operated independently by separate micromanipulators. Both electrodes were moved in unison toward the cell and punctured the presynaptic terminal about 50 to 100 μm from its distal end during monitoring of membrane potential. The outer microelectrode was then retracted, exposing the inner tip. Gigohm seals formed either spontaneously or in response to slight negative pressure. The polarities of potentials reported here refer to those of the patch pipette relative to that of the ground electrode, which was placed in the external medium. The sample rate was 20 kHz, and data were filtered at 500 to 1000 Hz.
18. E. A. Jonas *et al.*, data not shown.
19. Stimulation of the presynaptic nerve (at 20 Hz for 0.1 ms, then at 20 to 60 V for 1 to 10 s) was performed with an external suction electrode (*18*). For recordings of presynaptic action potentials and postsynaptic responses, both pre- and postsynaptic cells were impaled with recording electrodes according to conventional intracellular techniques [T. Dresbach *et al.*, *J. Neurosci.* **18**, 2923 (1998)].
20. D. Swandulla, M. Hans, K. Zipser, G. J. Augustine, *Neuron* **7**, 915 (1991).
21. D. Brdiczka, P. Kaldis, T. Wallimann, *J. Biol. Chem.* **269**, 27640 (1994).
22. L. Scorrano, V. Petronilli, P. Bernardi, *J. Biol. Chem.* **272**, 12295 (1997); L. M. Loew, W. Carrington, R. A. Tuft, F. S. Fay, *Proc. Natl. Acad. Sci. U.S.A.* **91**, 12579 (1994).
23. P. Bernardi *et al.*, *J. Biol. Chem.* **267**, 2934 (1992); Y. N. Antonenko, D. Smith, K. W. Kinnally, H. Tedeschi, *Biochim. Biophys. Acta* **1194**, 247 (1994).
24. V. Adams, W. Bosch, J. Schlegel, T. Wallimann, D. Brdiczka, *Biochim. Biophys. Acta* **981** 213 (1989).
25. Experiments were performed on small *Loligo pealei* at the Marine Biological Laboratory, Woods Hole, MA. Stellate ganglia were dissected according to the methods of R. Llinas *et al.* [R. Llinas, I. Z. Steinberg, K. Walton, *Biophys. J.* **33**, 289 (1981)] and G. J. Augustine and R. Eckert [*J. Physiol.* (*London*) **346** 257 (1984)]. Isolated ganglia were placed in a Lucite chamber and pinned to Sylgard with fine cactus needles. The bathing solution (pH 7.2) contained the following: 466 mM NaCl, 54 mM $MgCl_2$, 11 mM $CaCl_2$, 10 mM KCl, 3 mM $NaHCO_3$, and 10 mM Hepes; a similar solution that did not contain calcium was also used. The solutions were cooled, oxygenated with a 99.5% O_2, 0.5% CO_2 mixture [M. P. Charlton and G. D. Bittner, *J. Gen. Physiol.* **72**, 471 (1978)], and perfused over the ganglia.

26. We thank C. Pearson of the University of Connecticut Central Electron Microscope Facility for SEM experiments, T. Eisen and S. Jonas for comments on the manuscript, and K. E. Kaczmarek for technical support. The electrophysiological experiments were carried out at the Marine Biological Laboratory (MBL), Woods Hole, MA. Supported by NIH grants to L.K.K. and a fellowship award from MBL to E.A.J.

17 May 1999; accepted 30 September 1999

References and Notes

[4] **Microdomains with High Ca ²⁺ Close to IP₃-Sensitive Channels That Are Sensed by Neighboring Mitochondria**
Rosario Rizzuto; Marisa Brini; Marta Murgia; Tullio Pozzan
Science, New Series, Vol. 262, No. 5134. (Oct. 29, 1993), pp. 744-747.
Stable URL:
http://links.jstor.org/sici?sici=0036-8075%2819931029%293%3A262%3A5134%3C744%3AMWHCCT%3E2.0.CO%3B2-D

[4] **Close Contacts with the Endoplasmic Reticulum as Determinants of Mitochondrial Ca ²⁺ Responses**
Rosario Rizzuto; Paolo Pinton; Walter Carrington; Frederic S. Fay; Kevin E. Fogarty; Lawrence M. Lifshitz; Richard A. Tuft; Tullio Pozzan
Science, New Series, Vol. 280, No. 5370. (Jun. 12, 1998), pp. 1763-1766.
Stable URL:
http://links.jstor.org/sici?sici=0036-8075%2819980612%293%3A280%3A5370%3C1763%3ACCWTER%3E2.0.CO%3B2-U

[22] **Physiological Cytosolic Ca ²⁺ Transients Evoke Concurrent Mitochondiral Depolarizations**
Leslie M. Loew; Walter Carrington; Richard A. Tuft; Fredric S. Fay
Proceedings of the National Academy of Sciences of the United States of America, Vol. 91, No. 26. (Dec. 20, 1994), pp. 12579-12583.
Stable URL:
http://links.jstor.org/sici?sici=0027-8424%2819941220%2991%3A26%3C12579%3APCCTEC%3E2.0.CO%3B2-M